厚生労働科学研究費補助金（肝炎等克服緊急対策研究事業）
研究分担報告書

HCV 関連遺伝子発現アデノウイルスベクターシステムの開発及び班員へのベクター供給

研究分担者　鐘ヶ江裕美　東京大学医科学研究所　助教

研究要旨：近年の C 型肝炎ウイルス(HCV)研究の進展により、HCV 感染に伴い変動する細胞内遺伝子が複数同定されている。これらの細胞内遺伝子についての詳細な研究において、肝臓細胞へ遺伝子を効率的に導入することが可能であるアデノウイルスベクター(AdV)は有用性が高い。しかし、従来応用されていた第 1 世代アデノウイルスベクター(FG-AdV)は、細胞遺伝子発現に影響を与えるウイルス随伴 RNA (VA RNA)の発現が残存していたため、HCV 関連細胞遺伝子の検討では VA RNA の影響を考慮する必要があった。本研究では、新規に開発した VA RNA を欠失した AdV（VA 欠失 AdV）作製法を応用して作製したベクターを用いて VA RNA が RNA 干渉機構を競合拮抗していたことを HCV に対する short-hairpin RNA (shRNA)を用いて証明し、VA 欠失 AdV の本研究における有用性を示すとともに、HCV 感染により誘導されるオートファジー関連遺伝子をノックダウンするための ZFN を短期間のみ発現する AdV を作製し共同研究者に供与した。

A. 研究目的

C 型肝炎の病態の解明を行うためには、例えば HCV の複製を促進する miR122 などを発現あるいは細胞での発現をノックアウトする技術が必要である。本研究では肝臓への導入効率が高いアデノウイルスベクター（AdV）を用いた研究目的に則した発現機構を備えた AdV 開発を行う。AdV にはウイルス由来の VA RNA 発現が残存していたが、新規に開発された VA 欠失 AdV を応用することにより RNA 干渉機構を阻害しないシステムの応用が可能となっており、VA 欠失 AdV による shRNA や miRNA 発現を行っていく。また、ZFN や TALEN による細胞遺伝子発現のノックアウトを行うために、ZFN や TALEN を短期間高発現するシステムなどと組み合わせて最適化を図る。

B. 研究方法

VA 欠失 AdV による RNA 干渉機構への影響を判定するために、HCV の 5'非翻訳領域に対する short-hairpin RNA(shRNA)を 2 種類設定し、VA RNA を保持している従来の AdV と VA 欠失 AdV を作製した。コントロールとしてタカラバイオ社のスクランブル RNA (NC)を、陽性コントロールとしてインターフェロンを発現する VA 欠失あるいは保持 AdV を作製し実験に供した。VA 欠失 AdV は前川らの報告した方法に則って作製した。これらの AdV を HCV の遺伝子型 1b と 2a のレプリコン細胞に導入し、３日後に細胞を回収し、HCV ゲノムコピー数を 5'非翻訳領域に設定したプライマー／プローブを用いたリアルタイム PCR(qPCR)で定量した。また、JFH-1 感染細胞を用いて同様の検討を行い、HCV ゲノムコピー数を定量するとともに HCV 蛋白質の発現量を Western Blotting により評価した。HCV 感染により変動する複数の細胞遺伝子をノックアウトするための ZFN を発現するアデノウイルスベクターは、部位特異的組換え酵素 Cre 依存的に切り出された環状分子上で初めて発現する「切り出し発現型」として定法に従って構築した。

(倫理面への配慮)

本年度の研究に当たっては、既に実用化されているレプリコン細胞を用いた検討や培養細胞内の公表された遺伝子に対して設定された ZFN を発現するベクター作製であり、特に倫理面に抵触する検討は行っていない。

C. 研究結果

HCV に対する shRNA を発現するベクターを用いたレプリコン細胞を用いた解析から、本研究で設定した 2 種類の shRNA は遺伝子型 1b と

2a のいずれにおいても、陽性コントロールとして用いたインターフェロンよりは若干劣るものの、効率的に HCV ゲノム複製を抑制していたことが明らかになった。また、2 種類の shRNA は異なる場所に設定したため、この 2 種類の shRNA 発現 AdV を共感染した場合に最も高い HCV ゲノム複製抑制効果を示した。
VA RNA は、shRNA や miRNA と同様の機序を用いて細胞内でプロセスされるため、shRNA や miRNA と競合拮抗する可能性は示唆されていたが、VA 欠失 AdV の作製が困難であったため証明されていなかった。本研究で作製した 2 種類の shRNA を発現する VA 欠失 AdV は、いずれにおいても VA RNA コード領域を保持している従来の AdV よりも高い HCV 複製抑制効率を示した。この傾向は JFH-1 感染細胞においても再現されるとともに、HCV の蛋白質レベルでも発現抑制が確認されたことから、VA RNA が shRNA の効果を減弱させていたことを明らかにした。この結果から、HCV に関連する miRNA として知られている miR122 を含む miRNA を発現するためには VA 欠失 AdV の有用性が高いと結論した。
また、ZFN や TALEN を発現する AdV については、ZFN や TALEN が細胞内で長期間保持されることは細胞株作製において問題となることが多い。AdV は一過性の発現ベクターではあるが、細胞内で比較的安定にベクターゲノムが保持されることが知られており、細胞増殖が無ければ 6 ヶ月間目的遺伝子が持続発現していたことが報告されている。そこで、本研究では「切り出し発現型 AdV」として共同研究者に供与することとした。これは、目的遺伝子の下流にプロモーターを配するという通常とは異なった順番で挿入した発現ユニットの両側に Cre の標的配列である loxP を配した「切り出し発現ユニット」を持つ AdV であり、Cre 発現 AdV と共感染すると loxP 間が環状に切り出され、その環状分子上で初めてプロモーターと目的遺伝子が順方向の結合し目的遺伝子が発現するシステムである。Cre により切り出された環状分子は生成後 2 日目に約 1/6 に減少するため、細胞に高効率に短期間高度発現する発現単位を挿入する方法として有用性が高く、共同研究者はこの AdV で発現する ZFN を用いた細胞株の取得に成功した。

D. 考察

本研究により、細胞遺伝子発現を OFF に制御するために応用されている shRNA や miRNA を発現するためには VA 欠失 AdV が有用であることが明らかになった。近年 VA RNA 自体が miRNA として機能して複数の細胞遺伝子発現を低下することが報告されており、HCV 関連細胞遺伝子の発現にも影響を与える可能性があるため、今後は全てのベクターを VA 欠失 AdV として供給する体制を整えた。また本研究で同定した shRNA は HCV ゲノム複製を効率的に抑制することが明らかになり、遺伝子治療用ベクターとしても有用性が高いと考える。
ベクター供給としては、ZFN 発現 AdV を「切り出し発現型 AdV」として作製することで特定遺伝子ノックアウト細胞の樹立化の効率化が図られたが、今後は CRISP/Cas9 システムなどへも応用を広げていく。

E. 結論

shRNA や miRNA の発現には従来の AdV ではなく、VA 欠失 AdV の有用性が高いことを明らかにし、今後の供給体制を整えた。
また ZFN、TALEN 発現には「切り出し発現型 AdV」の有用性が高いことを示した。

F. 健康危険情報

特になし。

G. 研究発表

1.論文発表

1 Pei Z, Shi G, Kondo S, Ito M, Maekawa A, Suzuki M, Saito I, Suzuki T and Kanegae Y. Adenovius vectors lacking virus-associated RNA expression enhance shRNA atctivity to suppress hepatitis C virus replication. Scientific Rep., 2013, 3, 3575.

2 Maekawa A., Pei Z., Suzuki M., Fukuda F., Kondo S., Saito I., and Kanegae Y. Efficient production of adenovirus vector lacking genes of virus-associated RNAs that disturb cellular RNAi machinery. Scientific Rep., 2013, 3, 1136.

2. 学会発表

1 近藤小貴、宿主 RNAi 経路に影響を与える virus-associated RNA を欠失したアデノウイルスベクターの高効率作製法、第 19 回日本遺伝子治療学会学術集会、岡山、7

月 4-6 日、2013

2 近藤小貴、アデノウイルスベクターから発現しているウイルス由来 miRNAs は細胞増殖関連遺伝子を制御する、第 72 回日本癌学会学術総会、横浜、10 月 3-5 日、2013

3 Zheng Pei, Aya Maekawa, Mariko Suzuki, Yumi Kanegae, Saki Kondo, Izumu Saito, Therapeutic strategy of HBV using VA-deleted adenovirus vectors dually expressing shRNA and interferon. 2013 International Meeting on Molecular Biology of Hepatitis B viruses, Fudan University, Shanghai, October 20-23, 2013.

4 Yumi Kanegae, Aya Maekawa, Zheng Pei, Mariko Suzuki, Saki Kondo, Izumu Saito, Dual-safe adenovirus vector lacking virus-associated RNA genes enhanced shRNA activity. The 21th European Society of Gene and Cell Therapy collaborative Congress 2013, Palacio Municipal de Congresos de Madrid, Madrid, October 25-28, 2013.

5 Saki Kondo, Aya Maekawa, Mariko Suzuki, Yumi Kanegae, Izumu Saito, First-generation adenovirus vector expresses viral-associated (VA) RNAs that disturb cellular gene expressions. The 21th European Society of Gene and Cell Therapy collaborative Congress 2013, Palacio Municipal de Congresos de Madrid, Madrid, October 25-28, 2013.

6 Aya Maekawa, Zheng Pei, Mariko Suzuki, Saki Kondo, Izumu Saito, Yumi kanegae, Very efficient production of adenovirus vector lacking genes of virus-associated RNAs that disturb cellular RNAi machinery: safer alternative to current vector. The European Society of Gene and Cell Therapy 2013 Annual Meeting, Palacio Municipal de Congresos, Spain/Madrid, Octber 25-28, 2013.

7 近藤小貴、アデノウイルスベクターから常に発現している virus-associated (VA) RNA は標的細胞内の遺伝子発現に影響を与える、第 61 回日本ウイルス学会学術集会、神戸、11 月 10-12 日、2013

8 鈴木まりこ、アデノウイルスベクターの目的遺伝子挿入領域と向きはベクター作製や発現効率に影響を与えるか：Dual 発現 vector 作製に向けた検討、第 61 回日本ウイルス学会学術集会、神戸、11 月 10-12 日、2013

9 近藤小貴、アデノウイルスベクターの問題点：ベクターがコードする Virus-associated (VA) RNA は宿主遺伝子発現に影響を与える、第 36 回日本分子生物学会年会、神戸、12 月 3-6 日、2013

10 裴崢、1 つの細胞に多数の DNA コピーを導入できるマルチコピーを保持したコスミドのトランスフェクションにおける有用性：B 型肝炎ウイルスゲノム複製研究への応用、第 36 回日本分子生物学会年会、神戸、12 月 3-6 日、2013

11 前川　文、細胞特異的長期発現持続型 mini-adenovirus vector (mini-AdV)の開発、第 36 回日本分子生物学会年会、神戸、12 月 3-6 日、2013

12 鈴木まりこ、E3 領域への目的遺伝子の挿入はアデノウイルスベクターの作製効率に影響を与えるか：ベクター／目的遺伝子キメラ mRNA の生成、第 36 回日本分子生物学会年会、神戸、12 月 3-6 日、2013

H. 知的所有権の出願・登録状況

特になし。

別紙 4
研究成果の刊行に関する一覧表

書籍
無し

雑誌

発表者氏名	論文タイトル名	発表誌名	巻号	ページ	出版年
Katoh H, Okamoto T, Fukuhara T, Kambara H, Morita E, Mori Y, Kamitani W, Matsuura Y.	Japanese Encephalitis Virus Core Protein Inhibits Stress Granule Formation through an Interaction with Caprin-1 and Facilitates Viral Propagation	J Virol	87	489-502	2013
Lee H, Komano J, Saitoh Y, Yamaoka S, Kozaki T, Misawa T, Takahama M, Satoh T, Takeuchi O, Yamamoto N, Matsuura Y, Saitoh T, Akira S.	Zinc-finger antiviral protein mediates retinoic acid inducible gene I-like receptor-independent antiviral response to murine leukemia virus	Proc Natl Acad Sci U S A	110	12379-12384	2013
Kimura T, Katoh H, Kayama H, Saiga H, Okuyama M, Okamoto T, Umemoto E, Matsuura Y, Yamamoto M, Takeda K.	Ifit1 inhibits Japanese encephalitis virus replication through binding to 5' capped 2'-O unmethylated RNA	J Virol	87	9997-10003	2013
Tripathi LP, Kambara H, Chen YA, Nishimura Y, Moriishi K, Okamoto T, Morita E, Abe T, Mori Y, Matsuura Y, Mizuguchi K.	Understanding the biological context of NS5A-host interactions in HCV infection: a network-based approach	J Proteome Res	12	2537-2551	2013
Shibata C, Kishikawa T, Otsuka M, Ohno M, Yoshikawa T, Takata A, Yoshida H, Koike K.	Inhibition of microRNA122 decreases SREBP1 expression by modulating suppressor of cytokine signaling 3 expression.	Biochem Biophys Res Commun	438	230-235	2013
Sato M, Tateishi R, Yasunaga H, Horiguchi H, Yoshida H, Matsuda S, Fushimi K, Koike K.	Acute liver disease in Japan: a nationwide analysis of the Japanese Diagnosis Procedure Combination database.	J Gastroenterol		doi:10.1007/s00535-013-0843-9	2013
Yotsuyanagi H, Ito K, Yamada N, Takahashi H, Okuse C, Yasuda K, Suzuki M, Moriya K, Mizokami M, Miyakawa Y, Koike K.	High levels of HBV after the onset lead to chronic infection in patients with acute hepatitis B.	Clin Infect Dis	57	935-942	2013
Sato M, Kato N, Tateishi R, Muroyama R, Kowatari N, Li W, Goto K, Otsuka M, Shiina S, Yoshida H, Omata M, Koike K.	IL28B minor allele is associated with a younger age of onset of hepatocellular carcinoma in patients with chronic hepatitis C virus infection.	J Gastroenterol		doi:10.1007/s00535-013-0826-x	2013
Ohki T, Tateishi R, Akahane M, Mikami S, Sato M, Uchino K, Arano T, Enooku K, Kondo Y, Yamashiki N, Goto T, Shiina S, Yoshida H, Matsuyama Y, Omata M, Ohtomo K, Koike K.	CT with hepatic arterioportography as a pretreatment examination for hepatocellular carcinoma patients: a randomized controlled trial.	Am J Gastroenterol	108	1305-1313	2013

Inoue Y, Tomiya T, Nishikawa T, Ohtomo N, Tanoue Y, Ikeda H, Koike K.	Induction of p53-Dependent p21 Limits Proliferative Activity of Rat Hepatocytes in the Presence of Hepatocyte Growth Factor.	PLoS One	8	e78346	2013
Hikita H, Enooku K, Satoh Y, Yoshida H, Nakagawa H, Masuzaki R, Tateishi R, Soroida Y, Sato M, Suzuki A, Gotoh H, Iwai T, Yokota H, Koike K, Yatomi Y, Ikeda H.	Perihepatic lymph node enlargement is a negative predictor for sustained responses to pegylated interferon-α and ribavirin therapy for Japanese patients infected with hepatitis C virus genotype 1.	Hepatol Res	43	1005-1012	2013
He G, Dhar D, Nakagawa H, Font-Burgada J, Ogata H, Jiang Y, Shalapour S, Seki E, Yost SE, Jepsen K, Frazer KA, Harismendy O, Hatziapostolou M, Iliopoulos D, Suetsugu A, Hoffman RM, Tateishi R, Koike K, Karin M.	Identification of liver cancer progenitors whose malignant progression depends on autocrine IL-6 signaling.	Cell	155	384-396	2013
Kishikawa T, Otsuka M, Yoshikawa T, Ohno M, Takata A, Shibata C, Kondo Y, Akanuma M, Yoshida H, Koike K.	Regulation of the expression of the liver cancer susceptibility gene MICA by microRNAs.	Sci Rep	3	2739	2013
Liu Y, Higashitsuji H, Higashitsuji H, Itoh K, Sakurai T, Koike K, Hirota K, Fukumoto M, Fujita J.	Overexpression of gankyrin in mouse hepatocytes induces hemangioma by suppressing factor inhibiting hypoxia-inducible factor-1 (FIH-1) and activating hypoxia-inducible factor-1.	Biochem Biophys Res Commun	432	22-27	2013
Uchino K, Tateishi R, Nakagawa H, Shindoh J, Sugawara Y, Akahane M, Shibahara J, Yoshida H, Koike K.	Uninodular combined hepatocellular and cholangiocarcinoma with multiple non-neoplastic hypervascular lesions appearing in the liver of a patient with HIV and HCV coinfection.	J Clin Virol	57	173-177	2013
Ohno M, Shibata C, Kishikawa T, Yoshikawa T, Takata A, Kojima K, Akanuma M, Kang YJ, Yoshida H, Otsuka M, Koike K.	The flavonoid apigenin improves glucose tolerance through inhibition of microRNA maturation in miRNA103 transgenic mice.	Sci Rep	3	2553	2013
Ikeda K, Izumi N, Tanaka E, Yotsuyanagi H, Takahashi Y, Fukushima J, Kondo F, Fukusato T, Koike K, Hayashi N, Kumada H.	Fibrosis score consisting of four serum markers successfully predicts pathological fibrotic stages of chronic hepatitis B.	Hepatol Res	43	596-604	2013
Urabe Y, Ochi H, Kato N, Kumar V, Takahashi A, Muroyama R, Hosono N, Otsuka M, Tateishi R, Lo PH, Tanikawa C, Omata M, Koike K, Miki D, Abe H, Kamatani N, Toyota J, Kumada H, Kubo M, Chayama K, Nakamura Y, Matsuda K.	A genome-wide association study of HCV induced liver cirrhosis in the Japanese population identifies novel susceptibility loci at MHC region.	J Hepatol	58	875-882	2013

Hikita H, Nakagawa H, Tateishi R, Masuzaki R, Enooku K, Yoshida H, Omata M, Soroida Y, Sato M, Gotoh H, Suzuki A, Iwai T, Yokota H, Koike K, Yatomi Y, Ikeda H.	Perihepatic lymph node enlargement is a negative predictor of liver cancer development in chronic hepatitis C patients.	J Gastroenterol	48	366-373	2013
Tateishi R, Shiina S, Akahane M, Sato J, Kondo Y, Masuzaki R, Nakagawa H, Asaoka Y, Goto T, Otomo K, Omata M, Yoshida H, Koike K.	Frequency, risk factors and survival associated with an intrasubsegmental recurrence after radiofrequency ablation for hepatocellular carcinoma.	PLoS One	8	e59040	2013
Lo PH, Urabe Y, Kumar V, Tanikawa C, Koike K, Kato N, Miki D, Chayama K, Kubo M, Nakamura Y, Matsuda K.	Identification of a functional variant in the mica promoter which regulates mica expression and increases HCV-related hepatocellular carcinoma risk.	PLoS One	8	e61279	2013
Minami T, Kishikawa T, Sato M, Tateishi R, Yoshida H, Koike K.	Meta-analysis: mortality and serious adverse events of peginterferon plus ribavirin therapy for chronic hepatitis C.	J Gastroenterol	48	254-268	2013
Ikeda H, Enooku K, Ohkawa R, Koike K, Yatomi Y.	Plasma lysophosphatidic acid levels and hepatocellular carcinoma.	Hepatology	57	417-418	2013
Takata A, Otsuka M, Yoshikawa T, Kishikawa T, Hikiba Y, Obi S, Goto T, Kang YJ, Maeda S, Yoshida H, Omata M, Asahara H, Koike K.	MiRNA-140 acts as a liver tumor suppressor by controlling NF-κB activity via directly targeting Dnmt1 expression.	Hepatology	57	162-170	2013
Mawatari S, Uto H, Ido A, Nakashima K, Suzuki T, Kanmura S, Kumagai K, Oda K, Tabu K, Tamai T, Moriuchi A, Oketani M, Shimada Y, Sudoh M, Shoji I, Tsubouchi H.	Hepatitis C virus NS3/4A protease inhibits complement activation by cleaving complement component 4.	PLoS One	8	e82094	2013
Murakami Y, Fukasawa M, Kaneko Y, Suzuki T, Wakita T, Fukazawa H.	Retinoids and rexinoids inhibit hepatitis C virus independently of retinoid receptor signaling.	Microbes Infect	16	114-122	2013
Suzuki R, Matsuda M, Watashi K, Aizaki H, Matsuura Y, Wakita T, Suzuki T.	Signal peptidase complex subunit 1 participates in the assembly of hepatitis C virus through an interaction with E2 and NS2	PLoS Pathog	9	e1003589	2013

Matsumoto Y, Matsuura T, Aoyagi H, Matsuda M, Hmwe SS, Date T, Watanabe N, Watashi K, Suzuki R, Ichinose S, Wake K, Suzuki T, Miyamura T, Wakita T, Aizaki H.	Antiviral activity of glycyrrhizin against hepatitis C virus in vitro.	PLoS One	8	e68992	2013
Sakata K, Hara M, Terada T, Watanabe N, Takaya D, Yaguchi SI, Matsumoto T, Matsuura T, Shirouzu M, Yokoyama S, Yamaguchi T, Miyazawa K, Aizaki H, Suzuki T, Wakita T, Imoto M, Kojima S.	HCV NS3 protease enhances liver fibrosis via binding to and activating TGF-β type I receptor.	Sci Rep	3	3243	2013
Murakami Y, Fukasawa M, Kaneko Y, Suzuki T, Wakita T, Fukazawa H.	Selective estrogen receptor modulators inhibit hepatitis C virus infection at multiple steps of the virus life cycle.	Microbes Infect	15	45-55	2013
Saeed M, Gondeau C, Hmwe S, Yokokawa H, Date T, Suzuki T, Kato T, Maurel P, Wakita T.	Replication of hepatitis C virus genotype 3a in cultured cells.	Gastroenterology	144	56-58	2013
Yoshio, S., Kanto, T., Kuroda, S., Matsubara, T., Higashitani, K., Kakita, N., Ishida, H., Hiramatsu, N., Nagano, H., Sugiyama, M., Murata, K., Fukuhara, T., Matsuura, Y., Hayashi, N., Mizokami, M. and Takehara, T.	Human blood dendritic cell antigen 3 (BDCA3)(+) dendritic cells are a potent producer of interferon-lambda in response to hepatitis C virus.	Hepatology	57	1705-1715	2013
Oze, T., Hiramatsu, N., Yakushijin, T., Miyazaki, M., Iio, S., Oshita, M., Hagiwara, H., Mita, E., Inui, Y., Hijioka, T., Inada, M., Tamura, S., Yoshihara, H., Inoue, A., Imai, Y., Miyagi, T., Yoshida, Y., Tatsumi, T., Kanto, T., Kasahara, A., Hayashi, N. and Takehara, T.	Using early viral kinetics to predict antiviral outcome in response-guided pegylated interferon plus ribavirin therapy among patients with hepatitis C virus genotype 1.	J Gastroenterol		doi:10.1007/s00535-013-0824-z	2013
Ishida, H., Kato, T., Takehana, K., Tatsumi, T., Hosui, A., Nawa, T., Kodama, T., Shimizu, S., Hikita, H., Hiramatsu, N., Kanto, T., Hayashi, N. and Takehara, T.	Valine, the branched-chain amino acid, suppresses hepatitis C virus RNA replication but promotes infectious particle formation.	Biochem Biophys Res Commun	437	127-133	2013
Shen H, Yamashita A, Nakakoshi M, Yokoe H, Sudo M, Kasai H, Tanaka T, Fujimoto Y, Ikeda M, Kato N, Sakamoto N, Shindo H, Maekawa S, Enomoto N, Tsubuki M, Moriishi K	Inhibitory effects of caffeic Acid phenethyl ester derivatives on replication of hepatitis C virus	PLoS One	8	e82299	2013

Tani J, Shimamoto S, Mori K, Kato N, Moriishi K, Matsuura Y, Tokumitsu H, Tsuchiya M, Fujimoto T, Kato K, Miyoshi H, Masaki T, Kobayashi R	Ca(2+) /S100 proteins regulate HCV virus NS5A-FKBP8/FKBP38 interaction and HCV virus RNA replication., 33: 1008-1018, 2013	Liver Int	33,	1008-1018	2013
Ogawa Y, Kawamura T, Matsuzawa T, Aoki R, Gee P, Yamashita A, Moriishi K, Yamasaki K, Koyanagi Y, Blauvelt A, Shimada S	Antimicrobial Peptide LL-37 Produced by HSV-2-Infected Keratinocytes Enhances HIV Infection of Langerhans Cells	Cell Host Microbe	13	77-86	2013
Miura M, Maekawa S, Takano S, Komatsu N, Tatsumi A, Asakawa Y, Shindo K, Amemiya F, Nakayama Y, Inoue T, Sakamoto M, Yamashita A, Moriishi K, Enomoto N	Deep-Sequencing Analysis of the Association between the Quasispecies Nature of the Hepatitis C Virus Core Region and Disease Progression	J Virol	87	12541-12551	2013
Matsuzawa T, Kawamura T, Ogawa Y, Takahashi M, Aoki R, Moriishi K, Koyanagi Y, Gatanaga H, Blauvelt A, Shimada S	Oral administration of the CCR5 inhibitor, maraviroc, blocks HIV ex vivo infection of Langerhans cells within epithelium.	J Invest Dermatol	133	2803-2805	2013
Hashimoto K, Yamada S, Katano H, Fukuchi S, Sato Y, Kato M, Yamaguchi T, Moriishi K, Inoue N	Effects of immunization of pregnant guinea pigs with guinea pig cytomegalovirus glycoprotein B on viral spread in the placenta	Vaccine	31	3199-3205	2013
Aoki R, Kawamura T, Goshima F, Ogawa Y, Nakae S, Nakao A, Moriishi K, Nishiyama Y, Shimada S	Mast Cells Play a Key Role in Host Defense against Herpes Simplex Virus Infection through TNF-alpha and IL-6 Production	J Invest Dermatol	133	2170-2179	2013
Honda S, Miyagi H, Suzuki H, Minato M, Haruta M, Kaneko Y, Hatanaka KC, Hiyama E, Kamijo T, Okada T, Taketomi A.	RASSF1A methylation indicates a poor prognosis in hepatoblastoma patients.	Pediatr Surg Int	29	1147-52	2013
Wakayama K, Kamiyama T, Yokoo H, Kakisaka T, Kamachi H, Tsuruga Y, Nakanishi K, Shimamura T, Todo S, Taketomi A.	Surgical management of hepatocellular carcinoma with tumor thrombi in the inferior vena cava or right atrium	World J Surg Oncol	11	259	2013
Shibasaki S, Takahashi N, Toi H, Tsuda I, Nakamura T, Hase T, Minagawa N, Homma S, Kawamura H, Taketomi A.	Percutaneous transhepatic gallbladder drainage followed by elective laparoscopic cholecystectomy in patients with moderate acute cholecystitis under antithrombotic therapy	J Hepatobiliary Pancreat Sci		doi: 10.1002/jhbp.28	2013
Okada T, Honda S, Miyagi H, Kubota KC, Cho K, Taketomi A.	Liver fibrosis in prenatally diagnosed choledochal cysts.	J Pediatr Gastroenterol Nutr	57	e14	2013

Kamiyama T, Yokoo H, Furukawa J, Kurogochi M, Togashi T, Miura N, Nakanishi K, Kamachi H, Kakisaka T, Tsuruga Y, Fujiyoshi M, Taketomi A, Nishimura S, Todo S.	Identification of novel serum biomarkers of hepatocellular carcinoma using glycomic analysis.	Hepatology	57	2314-25	2013
Ijichi H, Shirabe K, Taketomi A, Yoshizumi T, Ikegami T, Mano Y, Aishima S, Abe K, Honda H, Maehara Y.	Clinical usefulness of (18) F-fluorodeoxyglucose positron emission tomography/computed tomography for patients with primary liver cancer with special reference to rare histological types, hepatocellular carcinoma with sarcomatous change and combined hepatocellular and cholangiocarcinoma.	Hepatol Res	43	481-7	2013
Shimada S, Kamiyama T, Yokoo H, Wakayama K, Tsuruga Y, Kakisaka T, Kamachi H, Taketomi A.	Clinicopathological characteristics and prognostic factors in young patients after hepatectomy for hepatocellular carcinoma.	World J Surg Oncol	11	52-8	2013
Taketomi A, Shirabe K, Muto J, Yoshiya S, Motomura T, Mano Y, Ikegami T, Yoshizumi T, Sugio K, Maehara Y.	A rare point mutation in the Ras oncogene in hepatocellular carcinoma.	Surg Today	43	289-92	2013
Mano Y, Aishima S, Fujita N, Tanaka Y, Kubo Y, Motomura T, Taketomi A, Shirabe K, Maehara Y, Oda Y.	Tumor-associated macrophage promotes tumor progression via STAT3 signaling in hepatocellular carcinoma.	Pathobiology	80	146-54	2013
Tao RR, Huang JY, Lu YM, Hong LJ, Wang H, Masood MA, Ye WF, Zhu DY, Huang Q, Fukunaga K, Lou YJ, Shoji I, Wilcox CS, Lai EY, Han F.	Nitrosative stress induces peroxiredoxin 1 ubiquitination during ischemic insult via E6AP activation in endothelial cells both in vitro and in vivo.	Antioxid & Redox Sign		doi: 10.1089/ars.2013.5381	2013
Mawatari S, Uto H, Ido A, Nakashima K, Suzuki T, Kanmura S, Kumagai K, Oda K, Tabu K, Tamai T, Moriuchi A, Oketani M, Shimada Y, Sudoh M, Shoji I, Tsubouchi H.	Hepatitis C virus NS3/4A protease inhibits complement activation by cleaving complement component 4.	PLoS One	8	e82094, 1-7	2013
Wahyuni TS, Tumewu L, Permanasari AA, Apriani E, Adianti M, Rahman A, Widyawaruyanti A, Lusida MI, Fuad A, Soetjipto, Nasronudin, Fuchino H, Kawahara N, Shoji I, Deng L, Aoki C, Hotta H.	Antiviral activities of Indonesian medicinal plants in the East Java region against hepatitis C virus.	Virol J	10	1-9	2013
Ichimura T, Taoka M, Shoji I, Kato H, Hatakeyama S, Isobe T, Hachiya N.	14-3-3 Proteins sequester a pool of soluble TRIM32 ubiquitin ligase to repress autoubiquitination and cytoplasmic body formation.	J Cell Sci	126	2014-2026	2013

El-Shamy A, Shindo M, Shoji I, Deng L, Okuno T, Hotta H.	Polymorphisms of the Core, NS3 and NS5A proteins of hepatitis C virus genotype 1b associate with development of hepatocellular carcinoma.	Hepatology	58	555-563	2013
Kimura T, Katoh H, Kayama H, Saiga H, Okuyama M, Okamoto T, Umemoto E, Matsuura Y, Yamamoto M, Takeda K.	Ifit1 Inhibits Japanese Encephalitis Virus Replication through Binding to 5' Capped 2'-O Unmethylated RNA.	J Virol	87	9997-10003	2013
Sasai M, Yamamoto M.	Pathogen Recognition Receptors: Ligands and Signaling Pathways by Toll-like Receptors.	Int Rev Immunol	32	116-133	2013
Satoh T, Kidoya H, Naito H, Yamamoto M, Takemura N, Nakagawa K, Yoshioka Y, Morii E, Takakura N, Takeuchi O, Akira S.	Critical role of Trib1 in differentiation of tissue-resident M2-like macrophages.	Nature	495	524-528	2013
Lundberg AM, Ketelhuth DF, Johansson ME, Gerdes N, Liu S, Yamamoto M, Akira S, Hansson GK.	Toll-like receptor 3 and 4 signalling through the TRIF and TRAM adaptors in haematopoietic cells promotes atherosclerosis	Cardiovasc Res	99	364-373	2013
Kamiyama N, Yamamoto M, Saiga H, Ma JS, Ohshima J, Machimura S, Sasai M, Kimura T, Ueda Y, Kayama H, Takeda K.	CREBH determines the severity of sulpyrine-induced fatal shock.	PLoS One	8	e55800	2013
Kusu T, Kayama H, Kinoshita M, Jeon SG, Ueda Y, Goto Y, Okumura R, Saiga H, Kurakawa T, Ikeda K, Maeda Y, Nishimura J, Arima Y, Atarashi K, Honda K, Murakami M, Kunisawa J, Kiyono H, Okumura M, Yamamoto M, Takeda K.	Ecto-Nucleoside Triphosphate Diphosphohydrolase 7 Controls Th17 Cell Responses through Regulation of Luminal ATP in the Small Intestine.	J Immunol	190	774-783	2013
Pei Z, Shi G, Kondo S, Ito M, Maekawa A, Suzuki M, Saito I, Suzuki T, Kanegae Y.	Adenovius vectors lacking virus-associated RNA expression enhance shRNA atctivity to suppress hepatitis C virus replication.	Sci Rep	3	3575	2013
Maekawa A, Pei Z, Suzuki M, Fukuda F, Kondo S, Saito I, Kanegae Y.	Efficient production of adenovirus vector lacking genes of virus-associated RNAs that disturb cellular RNAi machinery.	Sci Rep	3	1136	2013

JVI
Journals.ASM.org

Japanese Encephalitis Virus Core Protein Inhibits Stress Granule Formation through an Interaction with Caprin-1 and Facilitates Viral Propagation

Hiroshi Katoh,[a] Toru Okamoto,[a] Takasuke Fukuhara,[a] Hiroto Kambara,[a] Eiji Morita,[b] Yoshio Mori,[d] Wataru Kamitani,[c] Yoshiharu Matsuura[a]

Department of Molecular Virology,[a] International Research Center for Infectious Diseases,[b] and Global COE Program,[c] Research Institute for Microbial Diseases, Osaka University, Osaka, Japan; Department of Virology III, National Institute of Infectious Diseases, Tokyo, Japan[d]

Stress granules (SGs) are cytoplasmic foci composed of stalled translation preinitiation complexes induced by environmental stress stimuli, including viral infection. Since viral propagation completely depends on the host translational machinery, many viruses have evolved to circumvent the induction of SGs or co-opt SG components. In this study, we found that expression of Japanese encephalitis virus (JEV) core protein inhibits SG formation. Caprin-1 was identified as a binding partner of the core protein by an affinity capture mass spectrometry analysis. Alanine scanning mutagenesis revealed that Lys^{97} and Arg^{98} in the α-helix of the JEV core protein play a crucial role in the interaction with Caprin-1. In cells infected with a mutant JEV in which Lys^{97} and Arg^{98} were replaced with alanines in the core protein, the inhibition of SG formation was abrogated, and viral propagation was impaired. Furthermore, the mutant JEV exhibited attenuated virulence in mice. These results suggest that the JEV core protein circumvents translational shutoff by inhibiting SG formation through an interaction with Caprin-1 and facilitates viral propagation *in vitro* and *in vivo*.

In eukaryotic cells, environmental stresses such as heat shock, oxidative stress, UV irradiation, and viral infection trigger a sudden translational arrest, leading to stress granule (SG) formation (1). SGs are cytoplasmic foci composed of stalled translation preinitiation complexes and are postulated to play a critical role in regulating mRNA metabolism during stress via so-called "mRNA triage" (2). The initiation of SG formation results from phosphorylation of eukaryotic translation initiation factor 2α (eIF2α) at Ser^{51} by various kinases, including protein kinase R (PKR), PKR-like endoplasmic reticulum kinase (PERK), general control nonrepressed 2 (GCN2), and heme-regulated translation inhibitor (HRI), which are commonly activated by double-stranded RNA (dsRNA), endoplasmic reticulum (ER) stress, nutrient starvation, and oxidative stress, respectively. Phosphorylation of eIF2α reduces the amount of eIF2-GTP-tRNA complex and inhibits translation initiation, leading to runoff of elongating ribosomes from mRNA transcripts and the accumulation of stalled translation preinitiation complexes. Thus, SGs are defined by the presence of components of translation initiation machinery, including 40S ribosome subunits, poly(A)-binding protein (PABP), eIF2, eIF3, eIF4A, eIF4E, eIF4G, and eIF5. Then, primary aggregation occurs through several RNA-binding proteins (RBPs), including T-cell intracellular antigen-1 (TIA-1), TIA-1-related protein 1 (TIAR), and Ras-Gap-SH3 domain-binding protein (G3BP). These RBPs are independently self-oligomerized with the stalled initiation factors and with other RBPs, such as USP10, hnRNP Q, cytoplasmic activation/proliferation-associated protein-1 (Caprin-1), and Staufen and with nucleated mRNA-protein complex (mRNP) aggregations (3, 4). SG assembly begins with the simultaneous formation of numerous small mRNP granules which then progressively fuse into larger and fewer structures, a process known as secondary aggregation (5). The aggregation of TIA-1 or TIAR is regulated by molecular chaperones, such as heat shock protein 70 (Hsp70) (3), whereas that of G3BP is controlled by its phosphorylation at Ser^{149} (4). SG formation and disassembly in response to cellular stresses are strictly regulated by multiple factors.

Viral infection can certainly be viewed as a stressor for cells, and SGs have been reported in some virus-infected cells. Since the propagation of viruses is completely reliant on the host translational machinery, stress-induced translational arrest plays an important role in host antiviral defense. To antagonize this host defense, most viruses have evolved to circumvent SG formation during infection. For example, poliovirus (PV) proteinase 3C cleaves G3BP, leading to effective SG dispersion and virus propagation (6). Influenza A virus nonstructural protein 1 (NS1) has been shown to inactivate PKR and prevent SG formation (7). In the case of human immunodeficiency virus 1 (HIV-1) infection, Staufen1 is recruited in ribonucleoproteins for encapsidation through interaction with the Gag protein to prevent SG formation (8). In contrast, some viruses employ alternative mechanisms of translation initiation and promote SG formation to limit cap-dependent translation of host mRNA (9, 10). In addition, vaccinia virus induces cytoplasmic "factories" in which viral translation, replication, and assembly take place. These factories include G3BP and Caprin-1 to promote transcription of viral mRNA (11).

Japanese encephalitis virus (JEV) belongs to the genus *Flavivirus* within the family *Flaviviridae*, which includes other mosquito-borne human pathogens, such as dengue virus (DENV), West Nile virus (WNV), and yellow fever virus, that frequently cause significant morbidity and mortality in mammals and birds (12). JEV has

Received 15 August 2012 Accepted 15 October 2012
Published ahead of print 24 October 2012
Address correspondence to Yoshiharu Matsuura, matsuura@biken.osaka-u.ac.jp.

doi:10.1128/JVI.02186-12

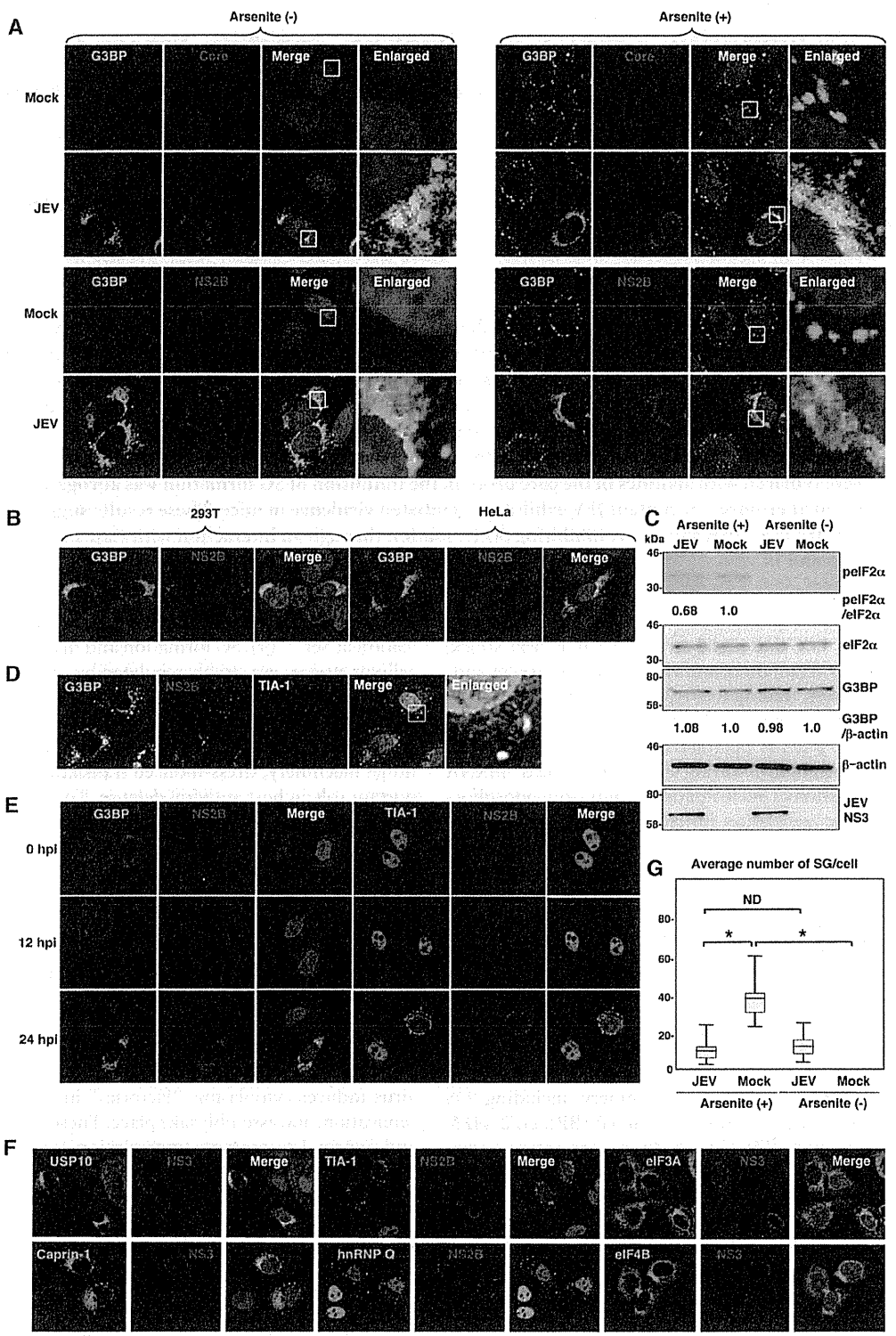

FIG 1 Dynamics of SG-associated factors during JEV infection. (A) Huh7 cells infected with JEV at an MOI of 0.5 were treated with or without 1.0 mM sodium arsenite for 30 min at 37°C, and the levels of expression of G3BP and JEV core protein/NS2B were determined at 24 h postinfection by immunofluorescence analysis with mouse anti-G3BP MAb and rabbit anti-core protein or anti-NS2B PAb, followed by AF488-conjugated anti-mouse IgG (Invitrogen) and AF594-conjugated anti-rabbit IgG, respectively. Cell nuclei were stained with DAPI (blue). (B) Cellular localizations of G3BP and JEV NS2B in 293T and HeLa cells infected with JEV were determined at 24 h postinfection by immunofluorescence analysis with mouse anti-G3BP MAb and rabbit anti-NS2B PAb, followed by AF488-conjugated anti-mouse IgG and AF594-conjugated anti-rabbit IgG, respectively. Cell nuclei were stained with DAPI (blue). (C) Phosphorylation of eIF2α in cells prepared as described in panel A was determined by immunoblotting using the indicated antibodies. The band intensities were quantified by ImageJ

a single-stranded positive-sense RNA genome of approximately 11 kb. The genomic RNA carries a single large open reading frame, and a polyprotein translated from the genome is cleaved co- and posttranslationally by host and viral proteases to yield three structural proteins, the core, precursor membrane (PrM), and envelop (E) proteins, and seven nonstructural (NS) proteins, NS1, NS2A, NS2B, NS3, NS4A, NS4B, and NS5 (13). PrM is further cleaved by the multibasic protease, furin, and matured to membrane (M) protein. The core, M, and E proteins are components of extracellular mature virus particles. NS proteins are not incorporated into particles and are thought to be involved in viral replication, which occurs in close association with ER-derived membranes (14). Previous reports have shown that WNV and DENV inhibit SG formation by sequestering TIA-1 and TIAR through specific interaction with viral RNA (15, 16). In addition, the membrane structure induced by WNV infection was suggested to prevent PKR activation and avoid induction of SG formation (17). In this study, we show that JEV core protein plays an important role in inhibition of SG formation. JEV core protein recruited several SG-associated proteins, including G3BP and USP10, through an interaction with Caprin-1 and suppressed SG formation. Furthermore, a mutant JEV carrying a core protein incapable of binding to Caprin-1 exhibited lower propagation *in vitro* and lower pathogenicity in mice than the wild-type (WT) JEV, suggesting that inhibition of SG formation by the core protein is crucial to antagonize host defense. These results reveal a novel strategy of JEV to inhibit SG formation through an interaction with Caprin-1 and facilitate viral propagation.

MATERIALS AND METHODS

Plasmids. Plasmids encoding FLAG-tagged JEV core protein (pCAGPM-FLAG-Core) and hemagglutinin (HA)-tagged JEV proteins (pCAGPM-HA-JEV proteins) were generated as previously described (18, 19). The cDNA of the core protein of JEV AT31 (amino acid residues 2 to 105) was amplified from the pCAGPM-FLAG-Core plasmid by PCR and cloned into pET21b (Novagen-Merck, Darmstadt, Germany) for expression in bacteria as a His-tagged protein and in pCAG-MCS2-FOS for expression in mammalian cells as a FLAG-One-STrEP (FOS)-tagged protein. The resulting plasmids were designated pET21b-Core-His and pCAG-Core-FOS, respectively. The cDNA of the core protein of DENV2 (amino acid residues 2 to 100) was amplified from the pCAG/FLAG-DEN2C-HA plasmid (19) by PCR and cloned into pCAGPM-N-FLAG. The cDNA of human Caprin-1 was amplified from 293T cells by reverse transcription-PCR (RT-PCR) and cloned into pCAGPM-N-HA (20) and pGEX 6P-1 (GE Healthcare, Buckinghamshire, United Kingdom) for expression in bacteria as a glutathione *S*-transferase (GST) fusion protein and designated pCAGPM-HA-Caprin-1 and pGEX-GST-Caprin-1, respectively. The cDNAs of human G3BP1 and USP10 were also amplified from 293T cells by RT-PCR and cloned into pCAGPM-N-HA. The nucleotide residues of the adenine at 384, adenine at 385, cytosine at 387, and guanine at 388 of the JEV genome in pMWATG1 were replaced with guanine, cytosine, guanine, and cytosine, respectively, by PCR-based mutagenesis to change Lys^{97} and Arg^{98} of the core protein to Ala, yielding pMWAT/KR9798A. The cDNA of the mutant core protein was also cloned into pCAGPM-N-FLAG and pET21b. To generate stable cell lines expressing *Aequorea coerulescens* green fluorescent protein (AcGFP)-fused Caprin-1, the cDNA of human Caprin-1 was amplified by RT-PCR and cloned into pAcGFP N1 (Clontech, Mountain View, CA), and the Caprin-1-AcGFP gene was subcloned into the lentiviral vector pCSII-EF-RfA (21) and designated pCSII-EF-Caprin-1-AcGFP. All plasmids were confirmed by sequencing with an ABI Prism 3130 genetic analyzer (Applied Biosystems, Tokyo, Japan).

Cells and stress treatment. Mammalian cell lines, Vero (African green monkey kidney), 293T (human kidney), Huh7 (human hepatocellular carcinoma), and HeLa (human cervical carcinoma), were maintained in Dulbecco's modified Eagle's minimal essential medium (DMEM) (Sigma, St. Louis, MO) supplemented with 100 U/ml penicillin, 100 mg/ml streptomycin, nonessential amino acids (Sigma), and 10% fetal bovine serum (FBS). The mosquito cell line C6/36 (*Aedes albopictus*) was grown in Leibovitz's L-15 medium with 10% FBS. Huh7 cells were transduced with a lentiviral vector expressing Caprin-1-AcGFP and AcGFP and designated Huh7/Caprin-1-AcGFP and Huh7/AcGFP, respectively. For induction of SGs, cells were treated with sodium arsenite at a final concentration of 1.0 mM in the culture medium for 30 min prior to fixation or lysis of the cells. SG formation was defined morphologically by immunostaining using anti-SG-related factor antibodies described below. Cell viability was determined by using CellTiter-Glo (Promega, Madison, WI) according to the manufacturer's instruction.

Viruses. The wild-type and 9798A mutant of the JEV AT31 strain were generated by the transfection of pMWATG1 and pMWAT/KR9798A, respectively, as described previously (22). Viral infectivity was determined by an immunostaining focus assay as described previously (20), and the results are expressed in focus-forming units (FFU). JEV and DENV serotype 2 New Guinea C strain were amplified in C6/36 cells.

Antibodies. Anti-JEV core rabbit polyclonal antibody (PAb) and anti-JEV NS3 mouse monoclonal antibody (MAb) were prepared as described previously (20, 23). Anti-JEV NS2B rabbit PAb was generated with synthetic peptides of JEV NS2B at Scrum, Inc. (Tokyo, Japan). Anti-DENV core protein rabbit PAb was prepared by using a GST-fused recombinant protein containing amino acid residues 2 to 100 of the DENV core protein. Anti-FLAG mouse MAb (M2) and rabbit PAb and anti-β-actin mouse MAb were purchased from Sigma. Anti-hnRNP Q mouse MAb (ab10687), anti-USP10 rabbit PAb (ab70895), and anti-eIF4B rabbit PAb (ab78916) were purchased from Abcam (Cambridge, United Kingdom). Anti-eIF2α, anti-phospho-eIF2α, and anti-eIF3A rabbit PAbs were purchased from Cell Signaling Technology (Danvers, MA). Anti-HA mouse MAb (HA11), anti-HA rat MAb (3F10), anti-His mouse MAb, anti-GFP mouse MAb (JL-8), anti-JEV envelope protein mouse MAb (6B4A-10), anti-G3BP mouse MAb, anti-TIA-1 goat PAb, anti-Caprin-1 rabbit PAb, and anti-dsRNA mouse MAb were purchased from Covance (Richmond, CA), Roche (Mannheim, Germany), R&D Systems (Minneapolis, MN), Clontech, Chemicon (Temecula, CA), BD Biosciences (Franklin Lakes, NJ), Santa Cruz (Santa Cruz, CA), Proteintech (Chicago, IL), and Bio-

software (NIH, Bethesda, MD), and the relative levels for the indicated proteins are shown based on the level of the mock-infected cells. (D) Cellular localizations of G3BP, NS2B, and TIA-1 in Huh7 cells infected with JEV were determined at 24 h postinfection by immunofluorescence analysis with mouse anti-G3BP MAb, rabbit anti-NS2B PAb, and goat anti-TIA-1 PAb, followed by AF488-conjugated anti-mouse IgG, AF594-conjugated anti-rabbit IgG, and AF633-conjugated anti-goat IgG, respectively. Cell nuclei were stained with DAPI (gray). (E) Dynamics of G3BP and TIA-1 during JEV infection. Huh7 cells infected with JEV were immunostained at 0, 12, and 24 h postinfection (hpi) with mouse anti-G3BP MAb or goat anti-TIA-1 PAb and rabbit anti-NS2B PAb, followed by AF488-conjugated anti-mouse IgG or AF488-conjugated anti-goat IgG and AF594-conjugated anti-rabbit IgG, respectively. Cell nuclei were stained with DAPI (blue). (F) Cellular localization of SG-associated proteins (USP10, Caprin-1, TIA-1, hnRNP Q, eIF3A, and eIF4B) (green, AF488-conjugated secondary antibody) and JEV NS2B/NS3 (red, AF-594-conjugate secondary antibody) in Huh7 cells infected with JEV was determined by immunoblotting at 24 h postinfection. Cell nuclei were stained with DAPI (blue). (G) Numbers of G3BP-positive foci in 30 cells prepared as described in panel A were counted for each experimental condition. Lines, boxes, and error bars indicate the means, 25th to 75th percentiles, and 95th percentiles, respectively. The significance of differences between the means was determined by a Student's *t* test.*, $P < 0.01$; ND, no significant difference.

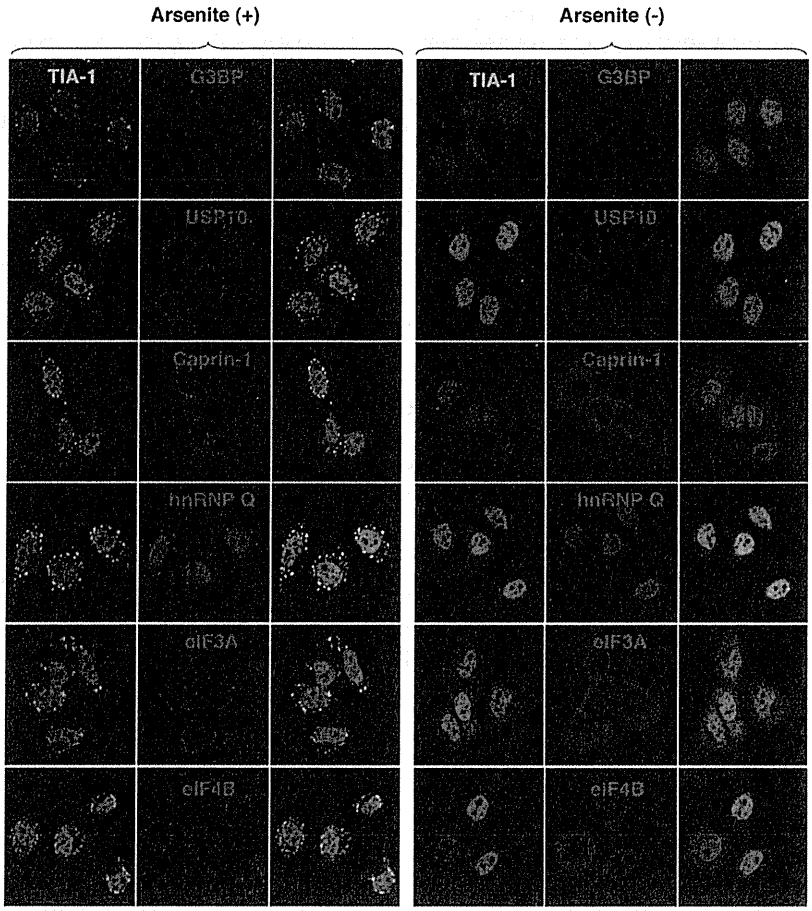

FIG 2 Each SG-associated factor forms SGs under oxidative stress. After treatment with 1.0 mM sodium arsenite for 30 min at 37°C, Huh7 cells were subjected to immunofluorescence analysis with the indicated primary antibodies, followed by AF488-conjugated anti-goat IgG and AF594-conjugated anti-mouse or rabbit IgG. Cell nuclei were stained with DAPI (blue).

center (Szirak, Hungary), respectively. Alexa Fluor (AF)-conjugated secondary antibodies were purchased from Invitrogen (Carlsbad, CA).

Immunofluorescence microscopy. Huh7 cells were fixed in 4% paraformaldehyde in phosphate-buffered saline (PBS) for 15 min at room temperature. After cells were quenched for 10 min with PBS containing 50 mM ammonium chloride (NH_4Cl), they were permeabilized with 0.2% Triton X-100 in PBS for 10 min and blocked with PBS containing 2% bovine serum albumin (BSA) for 30 min at room temperature. The cells were then incubated with the antibodies indicated in the figure legends. Nuclei were stained with 4′,6′-diamidino-2-phenylindole (DAPI). The samples were examined by a Fluoview FV1000 laser scanning confocal microscope (Olympus, Tokyo, Japan).

Transfection, immunoprecipitation, and immunoblotting. Plasmids were transfected into 293T or Huh7 cells by use of TransIT LT1 (Mirus, Madison, WI), and cells collected at 24 h posttransfection were subjected to immunostaining, immunoprecipitation, and/or immunoblotting as described previously (24). The immunoprecipitates were boiled in sodium dodecyl sulfate (SDS) sample buffer and subjected to SDS-polyacrylamide gel electrophoresis (SDS-PAGE). The proteins were transferred to polyvinylidene difluoride membranes (Millipore, Bedford, MA) and incubated with the appropriate antibodies. The immune complexes were visualized with SuperSignal West Femto substrate (Thermo Scientific, Rockford, IL) and detected by use of an LAS-3000 image analyzer system (Fujifilm, Tokyo, Japan).

FOS-tagged purification and mass spectrometry. pCAG-Core-FOS or empty vector was transfected into 293T cells, harvested at 24 h posttransfection, washed with cold PBS, suspended in cell lysis buffer (20 mM Tris-HCl, pH 7.4, 135 mM NaCl, 1% Triton X-100, and protease inhibitor cocktail [Complete; Roche]), and centrifuged at 14,000 × *g* for 20 min at 4°C. The supernatant was pulled down using 50 μl of STrEP-Tactin Sepharose (IBA, Gottingen, Germany) equilibrated with cell lysis buffer for 2 h at 4°C. The affinity beads were washed three times with cell lysis buffer and suspended in 2× SDS-PAGE sample buffer. The proteins were subjected to SDS-PAGE, followed by Coomassie brilliant blue (CBB) staining using CBB Stain One (Nakalai Tesque, Kyoto, Japan). The gels were divided into 10 pieces, and each fraction was trypsinized and subjected to liquid chromatography-tandem mass spectrometry (LC-MS/MS) analysis to identify coimmunoprecipitated proteins. All of the proteins in gels were identified comprehensively, and the proteins detected in cells transfected with pCAG-Core-FOS but not in those with empty vector were regarded as candidates for binding partners of JEV core.

Gene silencing. A commercially available small interfering RNA (siRNA) pool targeting Caprin-1 (siGENOME SMARTpool, human Caprin1) and control nontargeting siRNA were purchased from Dharmacon (Buckinghamshire, United Kingdom) and transfected into 293T cells using Lipofectamine RNAiMAX (Invitrogen) according to the manufacturer's protocol.

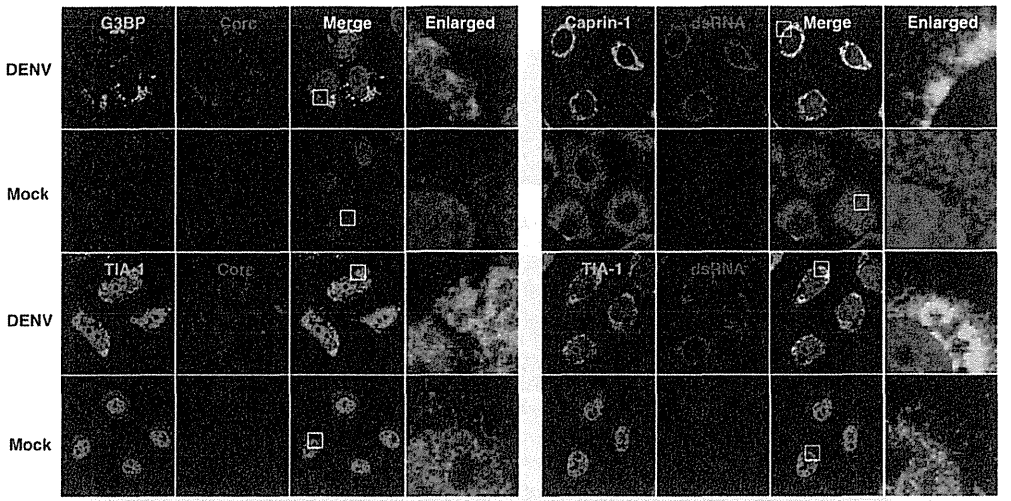

FIG 3 Subcellular localizations of the SG-associated proteins during DENV infection. Cellular localizations of G3BP, Caprin-1, and TIA-1 (green, AF488-conjugated secondary antibody) and viral components (core protein and dsRNA) (red, AF-594-conjugate secondary antibody) in Huh7 cells infected with DENV were determined by immunofluorescence analysis using the appropriate antibodies at 48 h postinfection. Cell nuclei were stained with DAPI (blue).

Preparation of recombinant proteins and GST pulldown assay. His-tagged JEV core protein (core-His) was purified as described in a previous report (25). Briefly, core-His was expressed in *Escherichia coli* (*E. coli*) Rosetta-gami 2(DE3) strain cells (Novagen-Merck) transformed with pET21b-Core-His (WT or 9798A). Bacteria grown to an optical density at 600 nm of 0.6 were induced with 0.5 mM isopropyl-β-D-thiogalactopyranoside (IPTG), incubated for 5 h at 37°C with shaking, collected by centrifugation at 6,000 × *g* for 10 min, lysed in 10 ml of bacteria lysis buffer (50 mM Tris-HCl, pH 7.4, 150 mM NaCl, 1 mM EDTA, 1% Triton X-100, and protease inhibitor cocktail [Complete; Roche]) by sonication on ice, and centrifuged at 10,000 × *g* for 15 min. The supernatant containing core-His was subjected to ammonium sulfate fractionation, followed by cation exchange chromatography with a HiTrap SP column (GE Healthcare). The eluted core-His recombinant protein was dialyzed with 50 mM Tris-HCl buffer containing 150 mM NaCl at 4°C overnight. GST-fused Caprin-1 (GST-Caprin-1) was expressed in *E. coli* BL21(DE3) cells transformed with pGEX-GST-Caprin-1. Bacteria grown to an optical density at 600 nm of 1.0 were induced with 0.1 mM IPTG, incubated for 5 h at 25°C with shaking, collected by centrifugation at 6,000 × *g* for 10 min, lysed in 10 ml of bacteria lysis buffer by sonication on ice, and centrifuged at 10,000 × *g* for 15 min. The supernatant was mixed with 200 μl of glutathione-Sepharose 4B beads (GE Healthcare) equilibrated with bacteria lysis buffer for 1 h at room temperature, and then the beads were washed five times with lysis buffer. Twenty micrograms of GST-Caprin-1 or GST was mixed with equal volumes of the purified core-His for 2 h at 4°C with gentle agitation. The beads were washed five times with bacteria lysis buffer and then suspended in SDS-PAGE sample buffer.

Mouse experiments. Experimental infections were approved by the Committee for Animal Experiment of RIMD, Osaka University (H19-2-0). Female ICR mice (3 weeks old) were purchased from CLEA Japan (Tokyo, Japan) and kept in specific pathogen-free environments. Groups of mice ($n = 10$) were intraperitoneally inoculated with 5×10^4 FFU (100 μl) of the viruses. The mice were observed for 3 weeks after inoculation to determine survival rates. To examine viral growth in the brain, 5×10^4 FFU of the viruses were intraperitoneally administered to the groups of mice ($n = 3$). At 7 days postinfection, mice were euthanized, and the cerebrums were collected. The infectious titers in the homogenates of the cerebrums were determined in Vero cells as described above.

RESULTS

JEV infection confers resistance to SG induction. To examine the formation of SGs in cells infected with JEV, Huh7 cells were infected with JEV at a multiplicity of infection (MOI) of 0.5, and the expression of JEV proteins and an accepted marker for SGs, G3BP, was determined by immunofluorescence analysis at 24 h postinfection. G3BP was mainly accumulated in the perinuclear region and partially colocalized with the JEV core protein, while only partial colocalization with the NS2B protein was also observed (Fig. 1A, left). In addition, a few small G3BP-positive foci were scattered in the cytoplasm. This accumulation of G3BP was observed in not only Huh7 cells but also other cell lines, i.e., 293T and HeLa cells, infected with JEV (Fig. 1B). However, the expression level of G3BP in cells infected with JEV was comparable to that in mock-infected cells (Fig. 1C). To further investigate SG induction by JEV infection, expression of TIA-1, another SG marker, was examined. Although accumulation of TIA-1 in the perinuclear region was not observed, a few TIA-1-positive foci were observed in the JEV-infected cells and were colocalized with G3BP and JEV NS2B, indicating that SG foci were induced in cells infected with JEV (Fig. 1D). The accumulation of G3BP and the aggregation of TIA-1, indicating SG formation, appeared at 24 h postinfection in accord with the expression of viral proteins (Fig. 1E). We further examined the dynamics of other SG-associated factors in cells infected with JEV. Each factor formed clear SGs in cells treated with sodium arsenite, a potent SG inducer eliciting oxidative stress (Fig. 2). As shown in Fig. 1F, three distinct patterns of the subcellular localization of SG components were observed. USP10 and Caprin-1 were accumulated in the perinuclear region and also formed a few small foci scattered throughout the cytoplasm, as seen for G3BP; TIA-1 and hnRNP Q formed cytoplasmic foci but were not accumulated in the perinuclear region; and subcellular localization of eIF3A and eIF4B was not changed. The cytoplasmic foci were confirmed as SGs by immunofluorescence analyses using specific antibodies to SG-associated factors (data not shown). Taken together, these results indicate that JEV infection induces accumulation of several RBPs and formation of a few SGs.

It has been shown previously that infection with WNV or DENV confers resistance to SG formation induced by sodium arsenite (15). To determine the effect of JEV infection on the SG

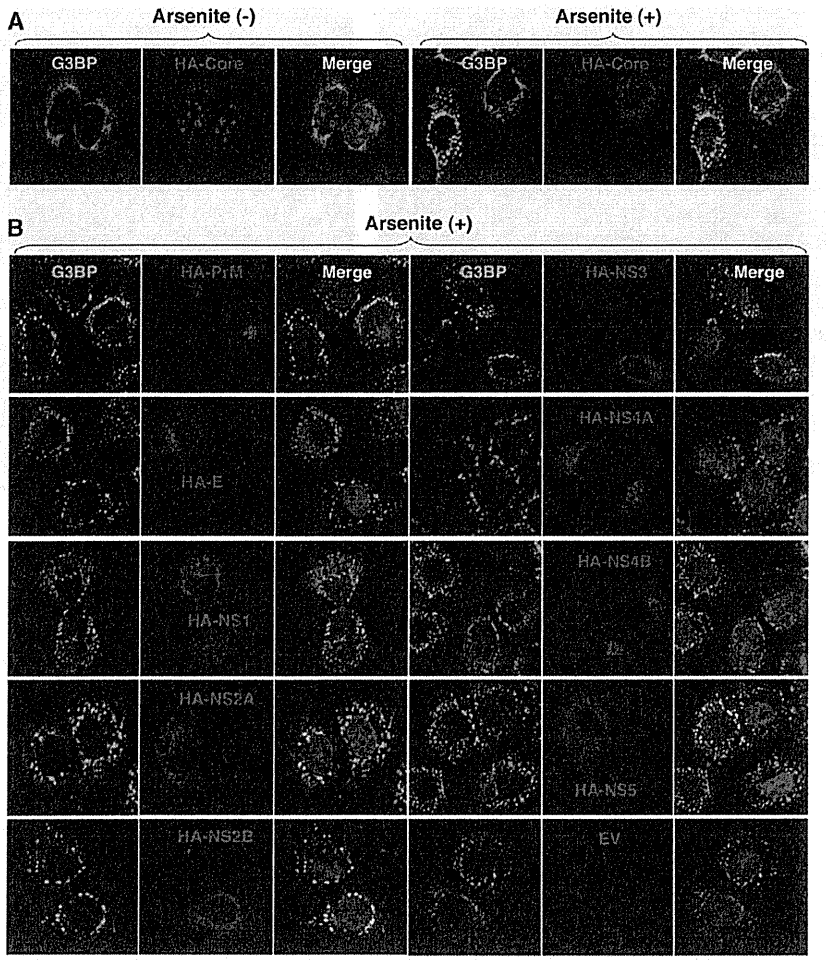

FIG 4 Inhibition of the arsenite-induced SG formation by the expression of JEV proteins. (A) Huh7 cells transfected with a plasmid, pCAGPM-HA-Core, were treated with or without 1.0 mM sodium arsenite for 30 min at 37°C, and the cellular localizations of G3BP and HA-Core were determined at 24 h posttransfection by immunofluorescence analysis with mouse anti-G3BP MAb and rat anti-HA MAb, followed by AF488-conjugated anti-mouse IgG and AF594-conjugated anti-rat IgG, respectively. Cell nuclei were stained with DAPI (blue). (B) Huh7 cells, which were separately transfected with a plasmid expressing an individual viral protein (pCAGPM-HA-JEV protein) as indicated in the figure, were treated with 1.0 mM sodium arsenite for 30 min at 37°C and subjected to an immunofluorescence assay using mouse anti-G3BP MAb and rat anti-HA MAb, followed by AF488-conjugated anti-mouse IgG and AF594-conjugated anti-rat IgG, respectively. Cell nuclei were stained with DAPI (blue).

formation induced by sodium arsenite, JEV-infected cells were treated with 0.5 mM sodium arsenite for 30 min at 24 h postinfection. Although many G3BP-positive foci were observed in mock-infected cells by the treatment with sodium arsenite, accumulation of G3BP in the perinuclear region was observed in the JEV-infected cells (Fig. 1A, right), and the numbers of G3BP-positive foci in the JEV-infected cells were less than those in the mock-infected cells (Fig. 1G). Although it has been reported that a significant reduction of the phosphorylation at Ser^{51} of eIF2α in cells treated with arsenite was induced by infection with WNV (15), the phosphorylation of eIF2α was slightly suppressed in the JEV-infected cells (Fig. 1C). Furthermore, while previous studies reported that Caprin-1 and TIA-1 were colocalized with dsRNA in cells infected with DENV (15, 26), no colocalization of G3BP or TIA-1 with the DENV core protein was observed in the present study (Fig. 3), suggesting that the mechanisms of the viral circumvention of SG formation in cells infected with JEV are different from those in cells infected with WNV and DENV.

JEV core protein suppresses SG formation induced by sodium arsenite. To elucidate the molecular mechanisms of suppression of SG formation induced by sodium arsenite during JEV infection, we tried to identify which viral protein(s) is responsible for the SG inhibition. Since G3BP was colocalized with JEV core protein, we first examined the involvement of the core protein in the perinuclear accumulation of G3BP and in the suppression of SG formation. The expression of JEV core protein alone induced the accumulation of G3BP in the perinuclear region (Fig. 4A, left panel) and suppressed sodium arsenite-induced SG formation (Fig. 4A, upper right cell in the right panel), similarly to JEV infection. In contrast, inhibition of SG formation induced by sodium arsenite was not observed in cells expressing other JEV proteins (Fig. 4B). These results suggest that JEV core protein is responsible for the circumvention of the SG formation observed in cells infected with JEV.

JEV core protein directly interacts with Caprin-1, an SG-associated cellular factor. Since JEV core protein was suggested to

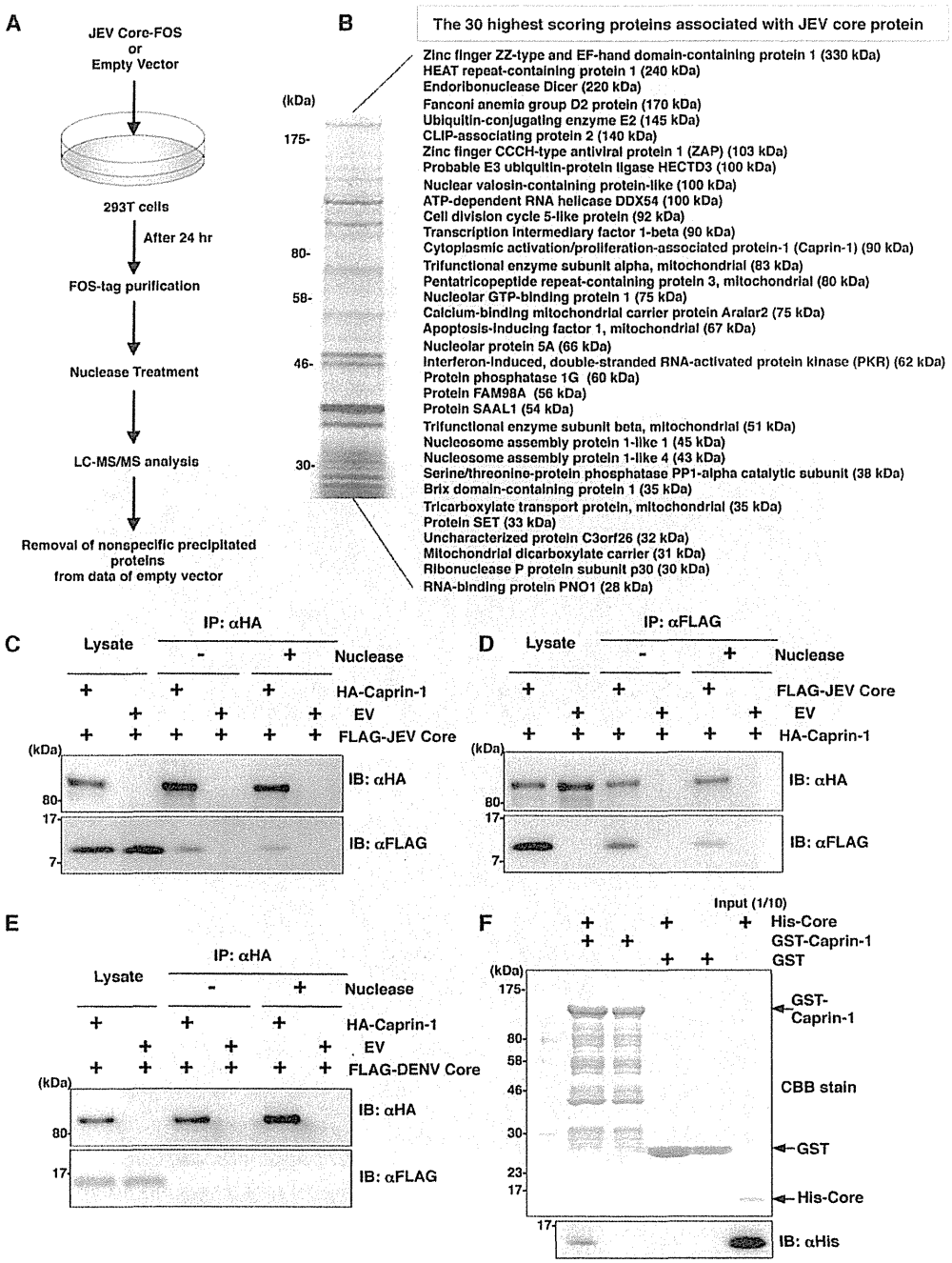

FIG 5 JEV core protein directly interacts with Caprin-1, an SG-associated cellular factor. (A) Identification of host cellular proteins associated with JEV core protein by FOS-tagged purification and LC-MS/MS analysis. Overview of the FOS-tagged purification of cellular proteins associated with JEV core protein. (B) The 30 candidate proteins as binding partners of JEV core protein exhibiting high scores are listed. PKR and Caprin-1 are indicated in red. (C and D) FLAG-JEV core protein and HA-Caprin-1 were coexpressed in 293T cells, and the cell lysates harvested at 24 h posttransfection were treated with or without micrococcal nuclease for 30 min at 37°C and immunoprecipitated (IP) with anti-HA (αHA) or anti-FLAG (αFLAG) antibody, as indicated. The precipitates were subjected to immunoblotting (IB) to detect coprecipitated counterparts. (E) FLAG-DENV core protein was coexpressed with HA-Caprin-1 in 293T cells, immunoprecipitated with anti-HA antibody, and immunoblotted with anti-HA or anti-FLAG antibody. (F) His-tagged JEV core protein was incubated with either GST-fused Caprin-1 or GST for 2 h at 4°C, and the precipitates obtained by GST pulldown assay were subjected to CBB staining and immunoblotting with anti-His antibody.

participate in the inhibition of SG formation, we tried to identify cellular factors associated with the core protein by LC-MS/MS analysis, as shown in Fig. 5A. Among the 30 factors with the best scores, two SG-associated proteins, PKR (Mascot search score, 206) and Caprin-1 (Mascot search score, 153), were identified as binding partners of JEV core protein (Fig. 5B). Although PABP1, hnRNP Q, Staufen, G3BP, and eIF4G were also identified, their scores were lower than those of PKR and Caprin-1. Because the

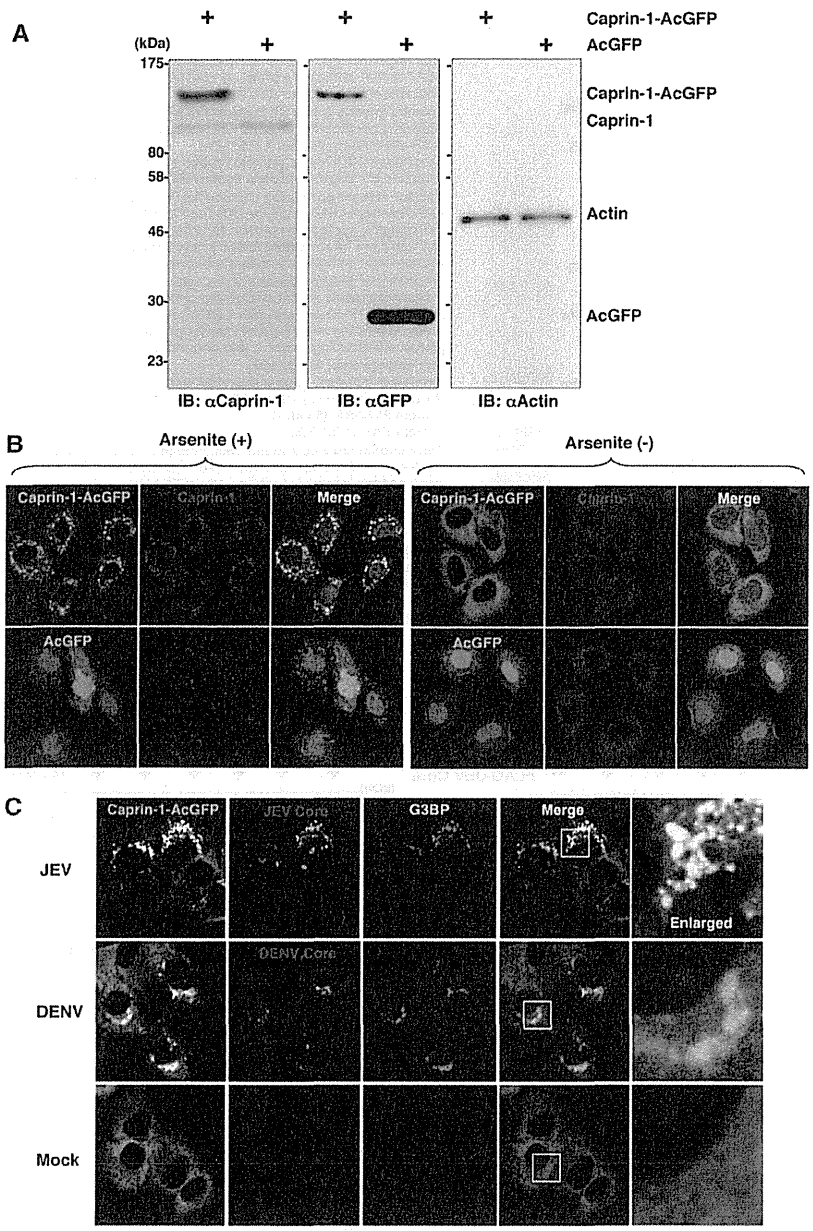

FIG 6 Caprin-1 is colocalized with the JEV core protein in the perinuclear region. (A) Expression of Caprin-1 fused with AcGFP (Caprin-1-AcGFP), Caprin-1, actin, or AcGFP in lentivirally transduced Huh7 cells was determined by immunoblotting using the appropriate antibodies. (B) Subcellular localization of Caprin-1-AcGFP or AcGFP (green) and endogenous Caprin-1 (red) in cells treated with/without 1.0 mM sodium arsenite for 30 min at 37°C was determined by immunofluorescence assay with rabbit anti-Caprin-1 PAb and AF594-conjugated anti-rabbit IgG. Cell nuclei were stained with DAPI (blue). (C) Huh7/Caprin-1-AcGFP cells were infected with either JEV or DENV at an MOI of 0.5, and the cellular localizations of JEV and DENV core (red) with Caprin-1-AcGFP and G3BP (blue) were determined at 24 h and 48 h postinfection, respectively. Cells were stained with mouse anti-G3BP MAb and rabbit anti-JEV or DENV core protein PAb, followed by AF633-conjugated anti-mouse IgG and AF594-conjugated anti-rabbit IgG, respectively, and examined by immunofluorescence analysis.

results shown in Fig. 1B suggest that the inhibition of SG formation takes place downstream of eIF2α phosphorylation, we focused on Caprin-1 as a key factor involved in the inhibition of SG formation in cells infected with JEV. To confirm the specific interaction of JEV core protein with Caprin-1, FLAG-JEV core protein and HA-Caprin-1 were coexpressed and immunoprecipitated with anti-HA or anti-FLAG antibody in the presence or absence of nuclease. FLAG-JEV core protein was coprecipitated with HA-Caprin-1 irrespective of nuclease treatment (Fig. 5C and D), suggesting that the interaction between JEV core protein and Caprin-1 is a protein-protein interaction. On the other hand, FLAG-DENV core protein was not coprecipitated with HA-Caprin-1 (Fig. 5E), indicating that the interaction with Caprin-1 was specific for JEV core protein. Next, the direct interaction be-

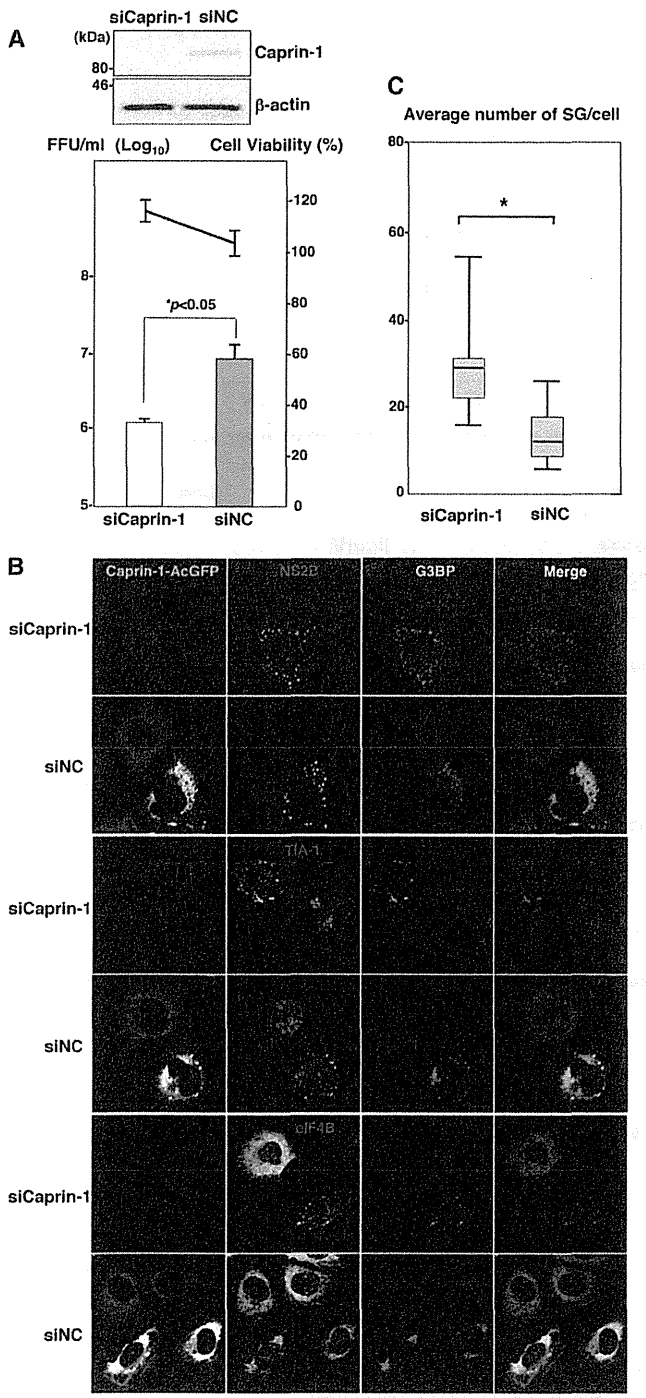

FIG 7 Knockdown of Caprin-1 cancels SG inhibition during JEV infection and suppresses viral propagation. (A) (Upper) The levels of expression of Caprin-1 in cells transfected with either siCaprin-1 or siNC was determined by immunoblotting using anti-Caprin-1 and anti-β-actin antibodies at 72 h posttransfection (top panel). At 48 h posttransfection with either siCaprin-1 or siNC, Huh7/Caprin-1-AcGFP cells were inoculated with JEV at an MOI of 0.5. At 24 h postinfection (72 h posttransfection), the infectious titers in the supernatants were determined by focus-forming assay in Vero cells (bottom panel, bar graph). Cell viability was determined at 72 h posttransfection and calculated as a percentage of the viability of cells treated with siNC (bottom panel, line graph). The results shown are from three independent assays, with the error bars representing the standard deviations. (B) At 48 h posttransfection with either siCaprin-1 or siNC, Huh7/Caprin-1-AcGFP cells were inoculated with JEV at an MOI of 0.5. The cellular localizations of SG-associated factors and JEV NS2B were determined at 24 h postinfection (72 h posttransfection) by immunofluorescence analysis with mouse anti-G3BP MAb and rabbit anti-NS2B PAb, rabbit anti-eIF4B PAb, or goat anti-TIA-1 PAb, followed by AF633-conjugated anti-mouse IgG and AF594-conjugated anti-rabbit IgG or AF594-conjugated anti-goat IgG, respectively. (C) Numbers of G3BP-positive foci in 30 cells prepared as described in panel B were counted. Lines, boxes, and error bars indicate the means, 25th to 75th percentiles, and 95th percentiles, respectively. The significance of differences between the means was determined by a Student's *t* test. *, $P < 0.01$.

tween JEV core protein and Caprin-1 was examined by a GST-pulldown assay using purified proteins expressed in bacteria. The His-tagged core protein was coprecipitated with GST-tagged Caprin-1, suggesting that JEV core protein directly interacts with Caprin-1 (Fig. 5F).

To further determine the cellular localization of Caprin-1 in JEV-infected cells, Caprin-1 fused with AcGFP (Caprin-1-AcGFP) was lentivirally expressed in Huh7 cells. The levels of expression and recruitment of Caprin-1-AcGFP into SGs were determined by immunoblotting and immunofluorescence analysis, respectively (Fig. 6A and B). In cells infected with JEV, Caprin-1-AcGFP was concentrated in the perinuclear region and colocalized with core protein and G3BP, while no colocalization of the proteins was observed in cells infected with DENV (Fig. 6C), suggesting that Caprin-1 directly interacts with JEV core protein in the perinuclear region of the infected cells.

Knockdown of Caprin-1 cancels SG inhibition during JEV infection and suppresses viral propagation. To assess the biological significance of the interaction of JEV core protein with Caprin-1 in JEV propagation, the expression of Caprin-1 was suppressed by using Caprin-1-specific siRNAs (siCaprin-1). Transfection of siCaprin-1 efficiently and specifically knocked down the expression of Caprin-1 with a slight increase of cell viability and decreased the production of infectious particles in the culture supernatants of cells infected with JEV, in comparison with those treated with a control siRNA (siNC) (Fig. 7A). Furthermore, immunofluorescence analyses revealed that knockdown of Caprin-1 increased the number of G3BP-positive granules colocalized with SG-associated factors, including TIA-1 and eIF4B, and inhibited the G3BP concentration in the perinuclear region (Fig. 7B and C). These results suggest that knockdown of Caprin-1 suppresses JEV propagation through the induction of SG formation.

Lys^{97} and Arg^{98} in the JEV core protein are crucial residues for the interaction with Caprin-1. To determine amino acid residues of the core protein that are required for the interaction with Caprin-1, we constructed a putative model based on the structural information of the DENV core protein previously resolved by nuclear magnetic resonance (NMR) (27), as shown in Fig. 8A. Based on this model, we selected hydrophobic amino acids, which were located on the solvent-exposed side in the α1 and α4 helices, as amino acid residues responsible for the binding to host proteins. Amino acid substitutions in each of the α-helices shown in Fig. 8B were designed in the context of FLAG-Core (Mα1 and Mα4), and the interaction of FLAG-Core mutants with Caprin-1 was examined by immunoprecipitation analysis. WT and Mα1, but not Mα4, core proteins were immunoprecipitated with Caprin-1 (Fig. 8B). To determine the amino acids responsible for interaction with Caprin-1, further alanine substitutions were introduced in the α4 helix, and the interaction was examined by immunopre-